

# TEM characterization of self-organized CdSe/ZnSe quantum dots

H. KIRMSE,\* R. SCHNEIDER,\* K. SCHEERSCHMIDT,† D. CONRAD† & W. NEUMANN\*

\*Humboldt-Universität zu Berlin, Institut für Physik, Lehrstuhl für Kristallographie,  
Invalidenstraße 110, D-10115 Berlin, Germany

†Max-Planck-Institut für Mikrostrukturphysik, Weinberg 2, D-06120 Halle, Germany

**Key words.** CdSe, digital image analysis, energy-dispersive X-ray spectroscopy, high-resolution transmission electron microscopy, image contrast simulation, molecular beam epitaxy, molecular dynamics, self-organized quantum dots, transmission electron microscopy, ZnSe.

## Summary

CdSe quantum dots (QDs) grown on ZnSe were investigated by various transmission electron microscopy (TEM) techniques including diffraction contrast imaging, high-resolution and analytical transmission electron microscopy both of plan-view as well as cross-section specimens. The size of the QDs ranges from about 5–50 nm, where from the contrast features in plan-view imaging two classes can be differentiated. In the features of the smaller dots there is no inner fine structure resolvable. The larger ones exhibit contrast features of fourfold symmetry as expected for pyramid-like islands. Corresponding simulations of diffraction contrast images of truncated CdSe pyramids with the edges of the basal plane orientated parallel to  $\langle 100 \rangle$  are in relatively good agreement with this assumption. In TEM diffraction contrast imaging of cross-section samples the locations of the quantum dots are visualized by additional dark contrast features. The QDs have a distinct larger extension in growth direction compared to the almost uniformly thick CdSe wetting layer. The presence of the CdSe QDs was also confirmed by energy-dispersive X-ray spectroscopy.

## Introduction

Semiconducting materials having structures of reduced dimensions in one, two or three spatial directions, e.g. quantum wells, quantum wires and quantum dots are characterized by promising particular optical and electronic properties owing to the charge carrier confinement. Nowadays, nanostructures such as quantum wires and quantum

dots (QDs) can be generated by self-organization phenomena like Stranski–Krastanow growth or spinoidal decomposition of strained structures. QDs in III–V as well as in II–VI semiconducting heterostructures described in the literature differ in size, morphology, structure and composition (Flack *et al.*, 1996; Lowisch *et al.*, 1996; Xin *et al.*, 1996; Hommel *et al.*, 1997; Ko *et al.*, 1997).

Transmission electron microscopical (TEM) investigations of structural properties of self-assembled CdSe QDs on ZnSe have recently been reported (Kirmse *et al.*, 1998). These QD structures were grown on (001) GaAs substrates by molecular beam epitaxy (MBE) using a modified growth regime (Rabe *et al.*, 1998), where after the deposition of three monolayers of CdSe the formation of QDs was initiated by thermal activation. In this paper, we report diffraction contrast studies and high-resolution electron microscopy (HRTEM) observations aimed at characterizing the size, morphology and structure of those CdSe QDs, and we discuss the experimental results in comparison with simulated diffraction contrast images of QD structure models relaxed by molecular dynamics. In addition, energy-dispersive X-ray spectroscopy (EDXS) was applied to detect the element contribution in the CdSe/ZnSe interfacial region using a small electron probe.

## Experimental procedure

The QD structures were grown by MBE on a (001) GaAs substrate. Three monolayers of CdSe were deposited onto a 1- $\mu\text{m}$  thick ZnSe buffer grown at 310°C, at a substrate temperature of 230°C. After that the substrate temperature was increased to the initial level and was held constant for a certain time, activating the formation of CdSe QDs. Finally, the structure was capped by 85 nm of ZnSe.

Correspondence to: Professor Dr Wolfgang Neumann, Humboldt-Universität zu Berlin, Institut für Physik/Kristallographie, Invalidenstraße 110, D-10115 Berlin, Germany. Tel: + 49 (0)30 20937761; fax: +49 (0)30 20937760; e-mail: wolfgang.neumann@physik.hu-berlin.de

For TEM examination the CdSe/ZnSe samples were prepared in plan-view as well as in cross-section. The plan-view samples were mechanically pre-thinned from the back to a thickness of about 100  $\mu\text{m}$ . Subsequently, they were dimpled on the back to a final thickness of approximately 30  $\mu\text{m}$ . Finally, ion milling ( $\text{Xe}^+$ ) was carried out applying a gradually reduction of the acceleration voltage to 0.7 kV. Both the use of  $\text{Xe}^+$  instead of  $\text{Ar}^+$  ions and the lowering of the voltage reduces the penetration depth of the ions and thus the thickness of the amorphous layer generated as an artefact (Chew & Cullis, 1987). In addition, the probability of defect generation is minimized (Wang & Fung, 1995). The preparation of cross-section samples comprised face-to-face glueing, drilling of cylinders out of the stack with the layers lying in the cylinder axis, cutting them into thin slices, polishing of both sides down to approximately 100  $\mu\text{m}$ , and finally dimpling and ion-milling.

TEM studies were performed on a Hitachi H-8110 and a Philips CM20 FEG, both operating at 200 kV. Energy-dispersive X-ray spectroscopical examinations were done by means of a Voyager system (Tracor Northern) attached to the Philips microscope, where EDXS line profiles were taken with an electron probe of 0.7 nm in diameter which was digitally controlled in the scanning TEM mode. At a microscope magnification of  $2 \times 10^6$  they were recorded across the different features of interest with the CdSe interlayer parallel to both the electron beam and to the X-ray detector axis. To adjust for an appropriate count statistics the specimen was tilted by about  $15^\circ$  to the detector. During X-ray analyses the specimen was kept at liquid nitrogen temperature via a Gatan double-tilt cooling holder (model 668) in order to minimize contamination.

### Molecular dynamics and contrast simulations

The relaxed atomic structures of the CdSe QDs in the ZnSe matrix are modelled by molecular dynamics simulations. Classical molecular dynamics (MD) provides a tool for simulating time dependent processes at an atomic level, e.g. the growth of crystals, the reordering of interfaces, and the relaxation of core structures of lattice defects. The equations of motion of an ensemble of particles are solved assuming suitable interatomic potentials and boundary conditions. The simulation of macroscopically relevant structures requires a large number of particles to be considered and many-body empirical potentials to be applied. The interatomic forces in covalent solids can be described completely only if the influence of the local environment according to the electronic structure is also included. However, empirical potentials have been developed; this allows one to simulate the non-local many-body interaction sufficiently well, thus enabling the application of long-time MD simulations

(10–100 ps) to larger systems as it is necessary to investigate, e.g. the relaxation of QDs. We have intensively tested different parameterizations of the Tersoff potential (Tersoff, 1989) and the Stillinger–Weber potential (Stillinger & Weber, 1985).

For the present calculations we applied our own parameterization of the Stillinger–Weber potential scaled with respect to the cohesive energy, the lattice constant, and the melting point similar to that of Wang *et al.* (1989) for the CdTe interaction. The pair interactions Cd–Se and Zn–Se are described completely, whereas intermixing of Cd and Zn is avoided by controlling the topology of the QDs. The starting configurations for our models are  $13 \times 13 \times 13$  supercells of ZnSe with 17 576 atoms in  $\{100\}$  orientation and the resulting box length is 7.31 nm. In  $\{110\}$  representation, necessary for comparing the simulations with the HRTEM investigations, the structure is changed by a  $\sqrt{2} \times \sqrt{2}/2 \times 1$  transformation. The CdSe QDs are inscribed as pyramidal-shaped islands of CdSe with (001) basal planes and 5 nm basal length, but having different possible crystallographic shapes. Different configurations are simulated, i.e. different side planes, truncated versus complete pyramids, and different principal axes of the basal plane as well as the axis of the supercell. The detailed discussion of the results will be published elsewhere. Here we restrict the considerations to truncated pyramids with the base axes along  $\langle 100 \rangle$  within the  $\{100\}$ -orientated supercell and with the base axes of the pyramid parallel to  $\langle 110 \rangle$  placed in the transformed supercell. Nevertheless, the energy differences and the atomic shifts between relaxed and unrelaxed structures are rather small (about 0.01 eV per atom). Characteristic strain fields inside and outside the pyramids are generated as a result of the lattice mismatch of about 7%.

In many cases the interpretation of diffraction contrast images as well as of HRTEM structure images requires the application of image matching techniques. Based on relaxed structure models image simulations were performed using the EMS software (Stadelmann, 1987) including the non-linear imaging process. The structures are sliced such that each slice contains only atoms with approximately the same coordinates in beam direction, which can be realized using 52 slices in plan-view imaging. The following parameters were applied to simulations of diffraction contrast bright-field images for a TEM Hitachi H-8110: accelerating voltage  $U = 200$  kV, spherical aberration  $c_s = 1.0$  mm, absorption potential factor  $q = 0.1$ , defocus spread  $\delta = 8$  nm, beam semi-convergence angle  $\alpha = 0.5$  mrad, and beam aperture  $\beta = 2.0\text{--}6.0$  nm $^{-1}$ . All thickness series were simulated with a defocus value of  $\Delta = 25$  nm lying between Gauss and Scherzer focus. As expected, and contrary to HRTEM simulations there is almost no contrast variation within a wide focus range. The thicknesses chosen are  $t = 7.4$ , 10.2 and 13.6 nm.

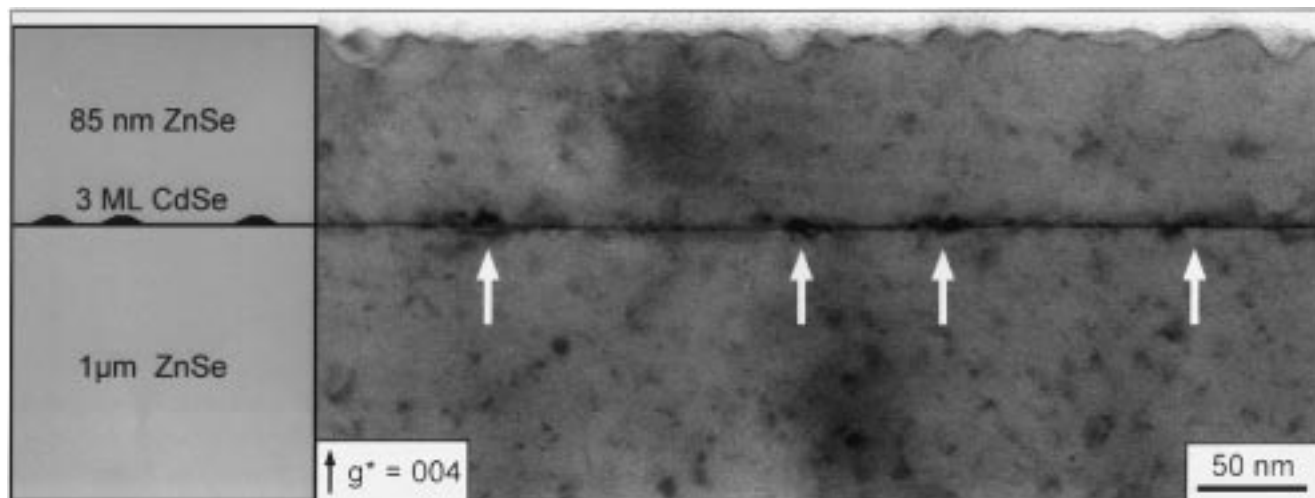


**Fig. 1.** Scheme of the sample set-up and corresponding cross-section TEM bright-field micrograph of the CdSe layer region (CdSe QDs marked by arrows).

### Results and discussion

The cross-section TEM investigations of the QD structures reveal the existence of an almost uniform wetting layer appearing as a dark narrow stripe within the adjacent ZnSe (cf. Fig. 1). The diffraction contrast image was taken with the 004 beam strongly excited to suppress contrast contributions arising from preparation artifacts in ZnSe. In the region of the CdSe wetting layer, which is almost free of defects, there are contrast features with a distinct wider extension in the growth direction, clearly indicating the positions of QDs. The mismatch between ZnSe and CdSe causes a strain field surrounding the QDs to have a strong influence on the diffraction contrast. The strain field permits only a rough estimate of the size of the QDs from these

images, yielding an average size of about 15 nm in width and about 5 nm in height. Moreover, on a small lateral scale there are slight changes of the thickness of the continuous dark line representing the wetting layer. This could be explained by lateral fluctuations in the strain field as well as in the chemical composition, which can be caused by alloying during ZnSe overgrowth (Rosenauer *et al.*, 1995).

Figure 2 shows an HRTEM image of a selected area of the wetting layer. The contrast behaviour of an individual QD is visible in the central part of the image. The cloud-like contrast is presumably due to the superposition of contributions caused by bent atom columns in the viewing direction and changes of the chemical composition (a detailed analysis using HRTEM image contrast simulations will be published elsewhere). The curvature of the atom

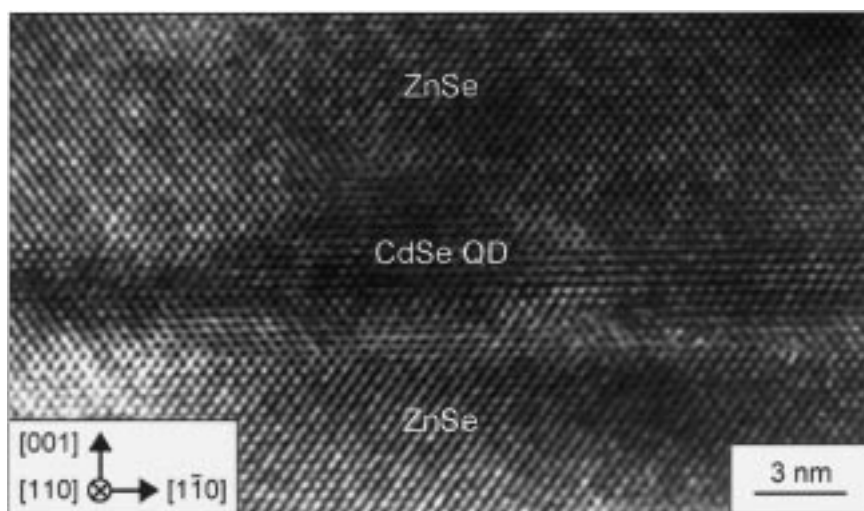


**Fig. 2.** HRTEM image of a single CdSe QD.

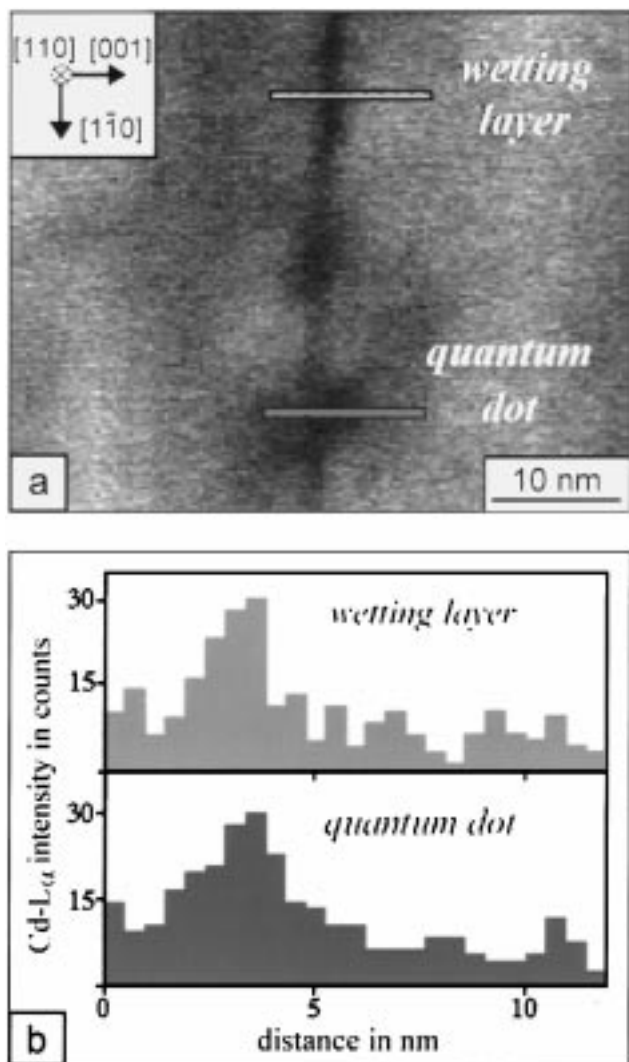


Fig. 3. EDXS analysis of the element distribution in the region of the CdSe layer: (a) STEM bright-field image, (b) imaging of the Cd distribution by EDXS line profiles.

columns is due to the strain field of the CdSe layer. A careful inspection of the experimental image exhibits an additional curvature of the  $\{111\}$  lattice planes in the QD region; thus an image analysis would provide information about the extension of the QDs.

The measurement of the distances of the Cd/Zn–Se columns in the  $\{111\}$  lattice planes of Fourier-filtered HRTEM images permits an estimate of the size of the entity causing the lattice distortion. Crossing the CdSe wetting layer the spacing is enlarged over 3 ML in comparison to the adjacent ZnSe, whereas across an outer region of a QD an increased spacing over 5 ML is found (Kirmse *et al.*, 1998).

To elucidate the distribution of the elements Zn, Cd and Se in the different zones of the CdSe layer, viz. solely the wetting layer and QD regions, EDXS line profiles were recorded across the different features of interest. In Fig. 3

the results are summarized for the Cd distribution. In the STEM bright-field image of Fig. 3(a) the wetting layer is represented by a straight vertical line on which two extra peculiarities of dark contrast, i.e. two QDs, are superimposed. Despite the low Cd concentration in the volume transmitted by the electron probe, the cadmium was detected by its Cd-L $\alpha$  line. Crossing the wetting layer step by step at c. 0.5 nm step width an average Cd extension of about 2.5 nm was found (cf. Fig. 3b), whereas it amounts about 5.5 nm for one single dot (see line drawn in Fig. 3a). Taking into account the deterioration of the information limit due to beam broadening and secondary fluorescence this result (thickness ratio of about 2.5/5.5 nm) is in good agreement with those of cross-section TEM and HRTEM investigations described above.

The size and the distribution of the ZnSe QDs were determined from TEM plan-view images. Figure 4 gives an overview revealing QDs of different sizes, where two classes of dot can be observed with respect to their contrast features. The larger ones show features with a diameter between 10 and 50 nm occurring with an area density of about  $20 \mu\text{m}^{-2}$ . Depending on the local orientation some of them show a fourfold symmetry, a hint of a pyramidal shape. TEM bright-field imaging of an individual QD (see Fig. 5a) with the 2–20 reflection strongly excited yields a fourfold symmetry of its contrast feature, too. The smaller contrast features in Fig. 4 with a lateral size between 5 and 10 nm appear with an area density of about  $100 \mu\text{m}^{-2}$ . These contrast features show no specific inner contrast according to their small sizes. Additionally, there seems to be a lateral alignment of the QDs in the  $\langle 110 \rangle$  directions, which is important for the formation of a QD grid resulting in improved optical properties of the quantum structure.

On the one hand the contrast features of the individual QD (see Fig. 5a) show a bright four-fold star with its spikes in the  $\langle 110 \rangle$  directions. This would suggest a pyramid with edges of the basal plane orientated parallel to  $\langle 100 \rangle$ . On the other hand, the corresponding diffraction pattern yields weak lines parallel to  $\langle 110 \rangle$  connecting the reflections (see Fig. 5b). From this fine structure it could be assumed that the pyramids are aligned with the edges of the basal plane parallel to  $\langle 110 \rangle$ . This alignment is known for the QDs of III-V semiconductors (Ruvimov & Scheerschmidt, 1995).

The two assumptions were checked by TEM bright-field contrast simulations. Inside the supercell shown in Fig. 6(a) a truncated CdSe pyramid with  $\{111\}$  facets is placed with the edges of the basal plane orientated parallel to  $\langle 110 \rangle$  according to the fine structure visible in the diffraction pattern. The supercell structure was recalculated by means of molecular dynamics structure relaxation based on a rescaled empirical Stillinger–Weber potential. Careful visual inspection reveals a curvature of the lattice planes in the area of the pyramid due to the relaxation as expected from strain field calculations of Ge(Si) islands grown on Si

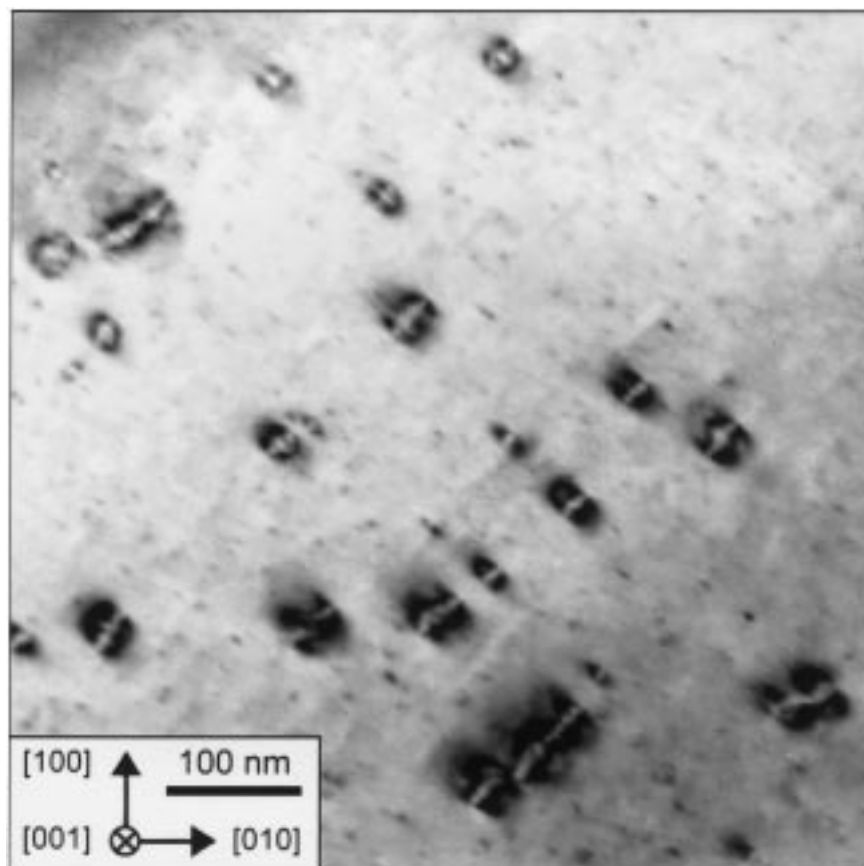


**Fig. 4.** Plan-view TEM bright-field image of the ZnSe/CdSe/ZnSe specimen.

(Christiansen *et al.*, 1994). Figure 6(b) presents the simulations of the plan-view bright-field contrast of the supercell for several thicknesses. The two images for a thickness of 13.6 nm are distinguished by the positions of the CdSe pyramid located near the electron beam entrance plane of the sample (left) and near the exit plane (right). The location of the pyramids within the supercell (near the entrance or the exit surface with respect to the electron beam) does not markedly influence the

contrast, probably because of the small slab thicknesses. However, one should be aware that the contrast is very sensitive to the sample thickness. A dark-bright contrast reversal could always be obtained in between the minimum and maximum thickness chosen in the simulations.

Contrary to the suggestion arising from the TEM bright-field contrast (see Fig. 5a), the simulation reveals a contrast feature having short bright spikes which are rotated by  $45^\circ$  around the [001] axis, excluding the alignment of the pyramid parallel to  $\langle 110 \rangle$ .

Figure 7(a) shows a truncated CdSe pyramid having  $\{110\}$  facets orientated parallel to  $\langle 100 \rangle$  within the elastically relaxed ZnSe supercell representing the conclusion from the TEM bright-field images. The results of the contrast simulations shown in Fig. 7(b) exhibit a good agreement with the experimental findings. Therefore, the CdSe QDs can be imagined as truncated pyramids with the edges of the basal plane aligned parallel to the  $\langle 100 \rangle$  directions and exhibiting  $\{110\}$  facets. The truncation height might slightly affect the extension of the bright central zone of the star-like pattern. However, since the simulation for complete pyramids gives contrast features

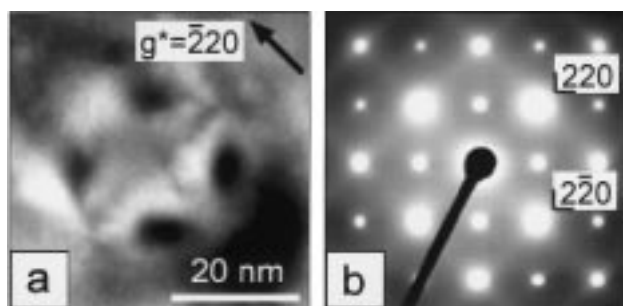


**Fig. 5.** (a) TEM bright-field image of an individual QD in plan-view and (b) corresponding selected-area electron diffraction pattern.

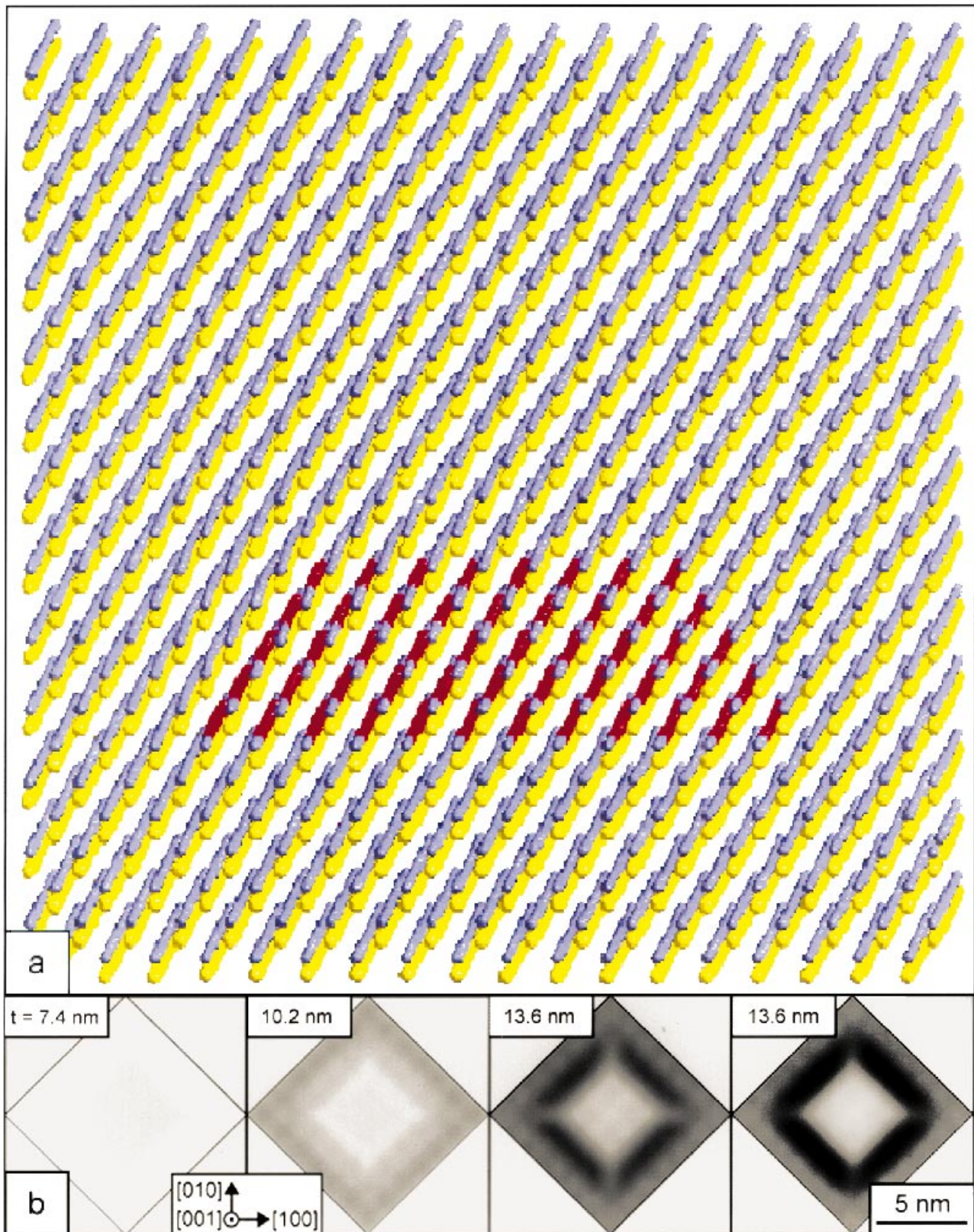


**Fig. 6.** Contrast simulation of TEM bright-field images of QD pyramids in plan-view: (a) side view of a relaxed supercell containing a truncated CdSe pyramid aligned with the edges of the basal plane parallel to the  $\langle 110 \rangle$  directions, (b) results of image contrast simulations for several thicknesses.

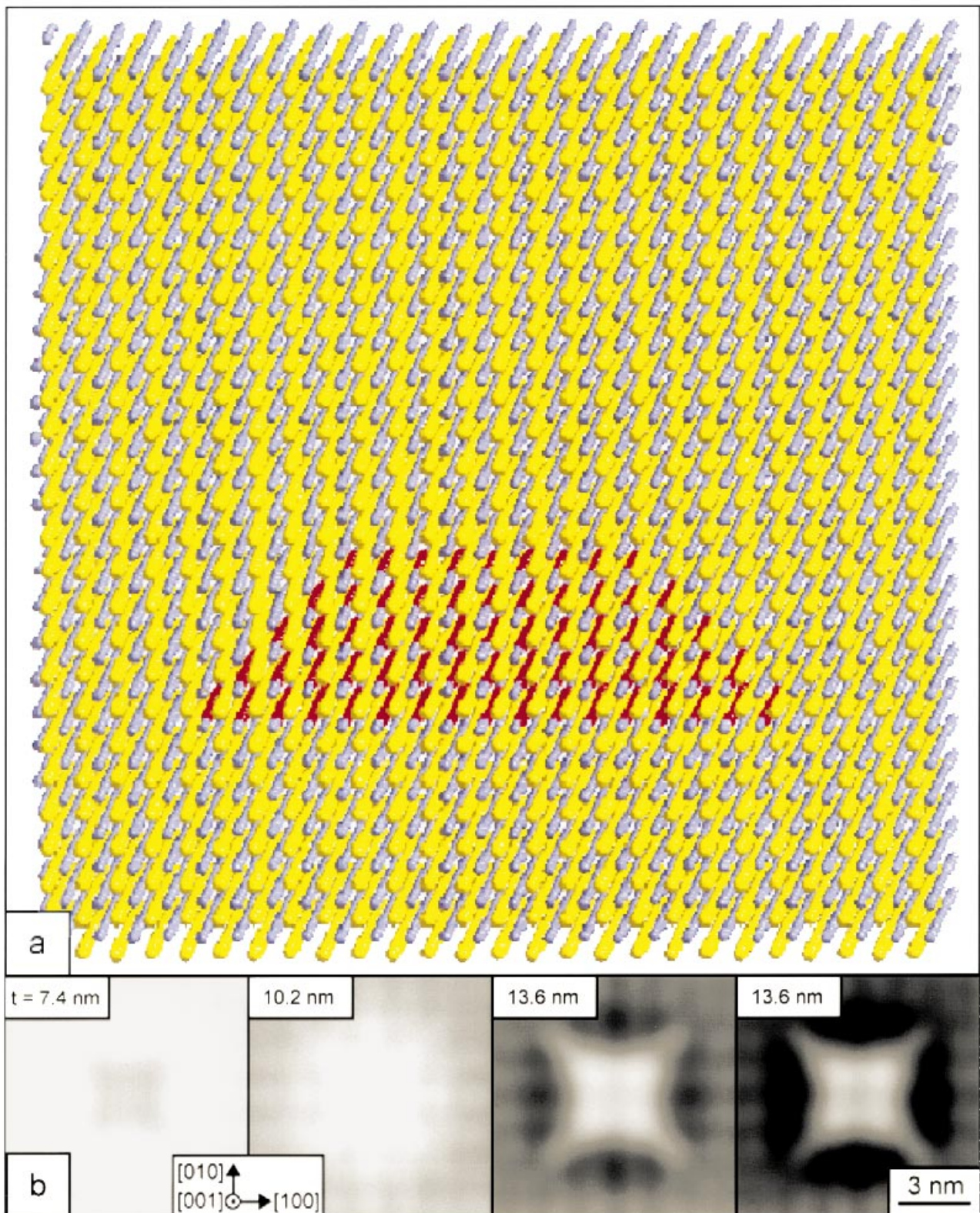


**Fig. 7.** Image contrast simulation (plan-view TEM) for a truncated CdSe pyramid orientated parallel to the  $\langle 100 \rangle$  directions: (a) side view of the pyramid embedded inside the supercell and (b) corresponding thickness series.

with a very narrow central zone the existence of such pyramids can be excluded.

The above-mentioned orientation of the CdSe pyramids is in contrast to that found for QD pyramids of III-V materials. One explanation of this difference might be the higher ionicity of CdSe in comparison to, e.g. (In,Ga)As making the nonpolar {110} facets more favourable than the polar {111} ones, i.e. neutral surfaces are predominantly expected to form contrary to charged ones for reasons of minimization of the surface energy.

## Conclusions

Diffraction contrast TEM imaging, HRTEM and EDXS analyses demonstrated the existence of CdSe QDs grown on ZnSe using a modified MBE growth regime. In cross-section TEM the QDs appear as dark contrast features with an average size of about 5 nm in height and about 15 nm in width that can be differentiated from the CdSe wetting layer visible as a continuous dark line of clearly smaller extension in growth direction. The presence of CdSe quantum dots was also confirmed by HRTEM cross-section imaging. Moreover, EDXS line profiles yielded a wider Cd distribution in dot regions in comparison with the adjacent layer, which additionally confirms the presence of CdSe QDs.

Plan-view TEM imaging revealed a statistical size distribution of the QDs from about 5–50 nm, whereas the existence of two classes of QDs was found with respect to their contrast features. The larger ones (about 10–50 nm in lateral size) show a contrast feature of fourfold symmetry, which cannot be observed for the smaller ones (c. 5–10 nm size) owing to their small extension. The comparison of the experimental images to bright-field contrast simulations of CdSe pyramids aligned parallel to different directions made the QDs appear as truncated pyramids with the edges of the basal plane orientated parallel to  $\langle 100 \rangle$  and having {110} facets. An important conclusion from the simulations is that the contrast feature of an elastically relaxed CdSe pyramid within ZnSe is not only influenced by the strain surrounding the pyramid embedded, but is also affected by the pyramid's shape and its orientation.

The results presented show that under certain MBE growth conditions relatively small QDs can also be generated for the II-VI system of CdSe/ZnSe, encouraging the growth of stacks of these structures in order to study their optical properties, and their lateral and vertical correlation.

## Acknowledgements

The authors are grateful to Professor F. Henneberger and

M. Rabe for supplying the QD structures. We would like to thank Professor U. Gösele for the provision of the CM 20 FEG at the Max Planck Institute of Microstructure Physics in Halle. H.K., R.S. and W.N. would also like to thank the Deutsche Forschungsgemeinschaft for financial support in the framework of the Sonderforschungsbereich 296. In addition, sincere thanks are due to the referees for their helpful comments.

## References

- Chew, N.G. & Cullis, A.G. (1987) The preparation of transmission electron-microscope specimens from compound semiconductors by ion milling. *Ultramicroscopy*, **23**, 175–198.
- Christiansen, S., Albrecht, M., Strunk, H.P. & Maier, H.J. (1994) Strained state of Ge (Si) islands on Si— finite-element calculations and comparison to convergent-beam electron-diffraction measurements. *Appl. Phys. Lett.* **64**, 3617–3618.
- Flack, F., Samarth, N., Nikitin, V., Crowell, P.A., Shi, J., Levy, J. & Awschalom, D.D. (1996) Near-field optical spectroscopy of localized excitons in strained CdSe quantum dots. *Phys. Rev.* **B54**, R17312–R17315.
- Hommel, D., Leonardi, K., Heinke, H., Selke, H., Ohkawa, K., Gindele, F. & Woggon, U. (1997) CdSe/ZnSe quantum dot structures – structural and optical investigations. *Phys. Stat. Sol. (b)*, **202**, 835–843.
- Kirmse, H., Schneider, R., Rabe, M., Neumann, W. & Henneberger, F. (1998) TEM investigations of structural properties of self-assembled CdSe/ZnSe quantum dots. *Appl. Phys. Lett.* **72**, 1329–1331.
- Ko, H.C., Park, D.C., Kawakami, Y. & Fuyita, S. (1997) Self organized CdSe quantum dots onto cleaved GaAs(110) originating from Stranski–Krastanow growth mode. *Appl. Phys. Lett.* **70**, 3278–3280.
- Lowisch, M., Rabe, M., Stegemann, B., Henneberger, F., Grundmann, M., Turck, V. & Bimberg, D. (1996) Zero-dimensional excitons in (Zn,Cd)Se quantum structures. *Phys. Rev.* **B54**, 11074–11077.
- Rabe, M., Lowisch, M. & Henneberger, F. (1998) Self-assembled CdSe quantum dots – formation by thermally activated surface reorganization. *J. Cryst. Growth*, **185**, 248–253.
- Rosenauer, A., Reisinger, T., Steinkirchner, E., Zweck, J. & Gebhardt, W. (1995) High resolution transmission electron-microscopy determination of Cd diffusion in CdSe/ZnSe single-quantum-well structures. *J. Cryst. Growth*, **152**, 42–50.
- Ruvimov, S. & Scheerschmidt, K. (1995) TEM/HRTEM visualization of nm-scale coherent InAs islands (quantum dots) in GaAs matrix. *Phys. Stat. Sol. (a)*, **150**, 471–478.
- Stadelmann, P.A. (1987) EMS – a software package for electron-diffraction analysis and HREM image simulation in materials science. *Ultramicroscopy*, **21**, 131–145.
- Stillinger, F.H. & Weber, T.A. (1985) Computer simulation of local order in condensed phases of silicon. *Phys. Rev.* **B31**, 5262–5271.

- Tersoff, J. (1989) Modelling solid-state chemistry – interatomic potentials for multicomponent systems. *Phys. Rev.* **B39**, 5566–5568.
- Wang, N. & Fung, K.K. (1995) Preparation of TEM plan-view and cross-sectional specimens of ZnSe/GaAs epilayers by chemical thinning and argon ion milling. *Ultramicroscopy*, **60**, 427–435.
- Wang, Z.Q., Stroud, D. & Markworth, A.J. (1989) Monte-Carlo study of the liquid CdTe surface. *Phys. Rev.* **B40**, 3129–3132.
- Xin, S.H., Wang, P.D., Yin, A., Kim, C., Dobrowolska, M., Merz, J.L. & Furdyna, J.K. (1996) Formation of self-assembling CdSe quantum dots on ZnSe by molecular-beam epitaxy. *Appl. Phys. Lett.* **69**, 3884–3886.